

AUTONOMOUS NAVIGATION IMPROVEMENTS FOR HIGH-EARTH ORBITERS USING GPS

Anne LONG, David KELBEL, and Taesul LEE

*Computer Sciences Corporation
Lanham-Seabrook, Maryland USA 20706*

James GARRISON and J. Russell CARPENTER

*NASA Goddard Space Flight Center
Greenbelt, Maryland USA 20771*

ABSTRACT – *The Goddard Space Flight Center is currently developing autonomous navigation systems for satellites in high-Earth orbits where acquisition of the GPS signals is severely limited. This paper discusses autonomous navigation improvements for high-Earth orbiters and assesses projected navigation performance for these satellites using Global Positioning System (GPS) Standard Positioning Service (SPS) measurements. Navigation performance is evaluated as a function of signal acquisition threshold, measurement errors, and dynamic modeling errors using realistic GPS signal strength and user antenna models. These analyses indicate that an autonomous navigation position accuracy of better than 30 meters root-mean-square (RMS) can be achieved for high-Earth orbiting satellites using a GPS receiver with a very stable oscillator. This accuracy improves to better than 15 meters RMS if the GPS receiver's signal acquisition threshold can be reduced by 5 dB-Hertz to track weaker signals.*

1 – INTRODUCTION

For the twenty-first century, National Aeronautics and Space Administration (NASA) Enterprises envision frequent low-cost missions to explore the solar system, observe the universe, and study our planet. Satellite autonomy is a key technology required to reduce satellite operating costs. The Guidance, Navigation, and Control Center (GNCC) at the Goddard Space Flight Center (GSFC) currently sponsors several initiatives associated with the development of advanced spacecraft systems to provide autonomous navigation and control.

Autonomous navigation has the potential both to increase spacecraft navigation system performance and to reduce total mission cost. By eliminating the need for routine ground-based orbit determination and special tracking services, autonomous navigation can streamline spacecraft ground systems. Autonomous navigation products can be included in the science telemetry and forwarded directly to the scientific investigators. In addition, autonomous navigation products are available onboard to enable other autonomous capabilities, such as attitude control, maneuver planning, orbit control, and communications signal acquisition. Autonomous navigation is required to support advanced mission concepts such as satellite formation flying.

GNCC has successfully developed high-accuracy autonomous navigation systems for near-Earth spacecraft using NASA's space and ground communications systems and the Global Positioning System (GPS) [Gram 94, Hart 97]. Recently, GNCC has expanded its autonomous navigation initiatives to include satellites in high-Earth orbits (HEOs), where the acquisition of GPS signals is

severely limited.

PiVoT (Position Velocity and Time), a GPS receiver being developed by the GNCC, is being developed for use as an improved navigation sensor in orbits with very high apogees. This receiver is intended to expand the range of missions for which GPS can be reliably used as the primary orbit determination sensor to encompass the wide range of orbit designs being considered for most future Earth-orbiting missions. Some enhancements to receiver architectures that are being studied include modified tracking loops to acquire and track the weaker side-lobe signals of the broadcast GPS satellites; tighter integration of a Kalman filter state estimator with the tracking loops; and improved search algorithms to account for this unusual orbital geometry.

The PiVoT receiver will host the GPS Enhanced Orbit Determination (GEODE) flight software. GEODE provides high accuracy navigation using an extended Kalman filter with realistic process noise models and a high-fidelity orbit propagator. High-fidelity Monte Carlo simulations have been performed to assess improvements in navigation accuracy achievable for eccentric high-Earth orbits and geosynchronous (GEO) orbits using GPS Standard Positioning System (SPS) pseudorange measurements. These simulations accurately model the GPS signal acquisition probability based on the GPS signal strength at the receiver, the user satellite's antenna characteristics, and the GPS receiver's acquisition threshold.

This paper discusses autonomous navigation improvements for HEOs and projected navigation performance for a 3×10 Earth radii orbit and a geosynchronous orbit. Navigation performance is evaluated as a function of signal acquisition threshold, measurement errors, and dynamic modeling errors using realistic GPS signal strength and user antenna models.

2 – OVERVIEW OF GPS NAVIGATION IMPROVEMENTS FOR HEO/GEO MISSIONS

GPS has been used extensively for satellites in low Earth orbit, and a few commercial receivers exist that can provide reliable and efficient onboard navigation solutions. In their current form, these receivers are not directly applicable to HEO and GEO missions because of important differences in the vehicle dynamics, signal levels, and geometrical coverage. To provide acceptable performance at high-Earth altitudes, some significant changes must be considered for existing GPS receiver architectures. The following improvements are needed for a GPS receiver intended for operation in HEO/GEO orbits:

- **Stable clock:** The need for an accurate and stable receiver clock increases because of the long periods of time when four GPS space vehicles (SVs) are not available simultaneously to produce a three-dimensional position and clock bias solution.
- **Robust navigation filter and clock model:** A capable and robust navigation filter and clock model is required to enable the receiver to generate solutions when fewer than four GPS SVs are visible simultaneously and to propagate a solution through GPS signal outages. The filter must support rapid reinitialization for missions that require frequent power cycling of the receiver to conserve power.
- **Satellite selection and signal acquisition:** Criteria other than dilution of precision (DOP) or highest elevation must be used to select and assign satellites to receiver channels for tracking. An estimate of received signal to noise ratio (C/N_0) should be one of the most important selection criteria. The signal acquisition algorithms may require mission specific customizations and must be robust enough to handle the varying conditions (Doppler, C/N_0 , etc.) experienced over each orbit. Furthermore, the search pattern used to vary code delay and Doppler frequency to look for new satellites must take into account the expected range of Doppler frequencies encountered in these orbits. One potential way to speed up this search is to assign multiple correlator channels to one GPS SV at different Doppler frequencies.

- Multiple antennas/channels: The changing geometric distribution of signals in the sky throughout an orbit requires multiple antennas and antenna orientations to provide the best coverage. The receiver should allow dynamic assignment of correlator channels to antennas to make the best use of the resources in the receiver as conditions change over the course of the mission or even during an orbit.
- High gain antennas: Certain nadir pointing spacecraft can utilize high gain receiving antennas to improve signal visibility at high altitudes.
- Weak signal tracking: Specific strategies can be employed to increase the number of GPS signals visible under certain conditions by better enabling the receiver to track weak GPS signals and to take advantage of available side lobe signals [Land 98]. Optimization of the tracking loop design for the expected dynamics of HEO and GEO can produce some improvement in tracking weaker GPS signals.
- Resistance to jamming: Receiver tracking loops must be resistant to jamming from other GPS SVs in close proximity, which periodically arises in HEO.
- Radiation tolerance: Through the selection of radiation hardened components, box level shielding, and upset tolerant software, the receiver must survive the extremely severe radiation environment in high altitude orbits.

[More 99] provides more information about the receiver architecture that GSFC is using for the PiVoT receiver. The remainder of this paper addresses the projected navigation performance of a GPS receiver designed to satisfy these requirements.

3 – PERFORMANCE SIMULATION PROCEDURE

To quantify the level of navigation performance that is achievable for high-Earth orbits, realistic simulations were performed for two representative missions as a function of receiver tracking threshold. The HEO test case is 3-Earth-radii by 10-Earth-radii, which is similar to one of the high altitude orbits proposed for the Magnetospheric Mapping mission and representative of the constellations of small satellites proposed under NASA’s Space Technology (ST) 5 project. The GEO test case is based on the GOES-10 orbit. Fig. 1 illustrates the location of the test orbits with respect to a single GPS SV broadcast signal.

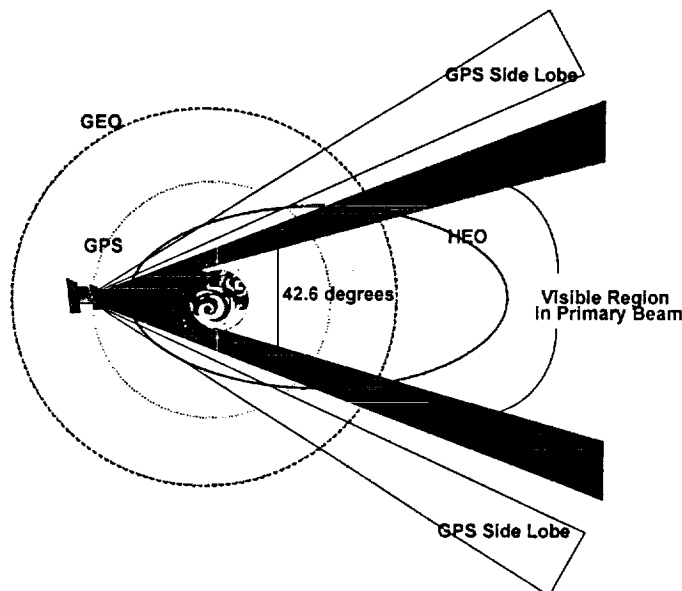


Fig. 1 Satellite Orbital Geometry With Respect to GPS Broadcast Signal

3.1 – Measurement Simulation

Realistic GPS pseudorange measurements were simulated for each HEO/GEO satellite using high-fidelity truth ephemerides and the measurement simulation options listed in Table 1. The truth ephemerides were generated using the Goddard Trajectory Determination System (GTDS) with the high-accuracy force model, which included a 70x70 Joint Goddard Model (JGM)-3 for nonspherical gravity forces, Jet Propulsion Laboratory Definitive Ephemeris 200 for solar and lunar gravitational forces, and solar radiation pressure forces. GTDS is the primary orbit determination program used for operational satellite support at GSFC.

The GPS constellation configuration was based on the GPS broadcast messages for the epoch date. The GPS signal strength at the GPS receiver's location was modeled assuming the nominal GPS Block II signal antenna pattern. The signal attenuation model that was used provides realistic signal acquisition predictions [More 99]. Three sets of pseudorange measurements were created for each sample orbit based on receiver signal-to-noise ratio acquisition thresholds of 35 dB-Hertz, 30 dB-Hertz, and 28 dB-Hertz.

Table 1. GPS Measurement Simulation Parameters

| Parameter | Value |
|--|--|
| Measurement data rate | Every 60 seconds from all visible GPS SVs |
| GPS SV ephemerides | Broadcast ephemerides for June 21-26, 1998 |
| GPS SV characteristics: | |
| SA errors | 25 meter (1-sigma) |
| Transmitting antenna pattern | GPS L-band pattern, modeled from 0 to 90 degrees down from boresight |
| Transmitted power | 28 dB-watts in maximum gain direction |
| User antenna models: | Hemispherical antenna (HEO): Maximum gain : 3.5dBic Horizon mask: 90 degrees from boresight High gain antenna (GEO): Maximum gain : 9.2dBic Horizon mask: 56 degrees from boresight |
| Visibility constraints | <ul style="list-style-type: none"> • Earth blockage with 50 km altitude tropospheric mask • GPS SV transmitting antenna beamwidth and receiving antenna horizon masks • Received signal-to-noise ratio above tracking threshold |
| GPS receiver characteristics | <ul style="list-style-type: none"> • Receiver noise figure: 2.9dB • System noise temperature: Earth-point antenna: 300K Otherwise: 180K • 12-channels, GPS SV signals selected based on highest signal-to-noise ratio • 35, 30, or 28 dB-Hertz receiver acquisition thresholds |
| Ionospheric delays | HEO: 90 meters below 250 km height 40 meters at 400 km height 8 meters at 1000 km GEO: 112 meters below 400 km height 10 meters at 1000 km |
| Receiver clock bias white noise spectral density | 9.616×10^{-20} seconds ² per second |
| Receiver clock drift rate white noise spectral density | 1.043×10^{-27} seconds ² per seconds ³ |
| Random pseudorange errors | 2 meters (1-sigma) |

Selective Availability (SA) measurement errors were applied at a 25-meter (1-sigma) level, using the Lear4 autoregressive integrated moving average time series model [JSC 93]. In the case of signals with long paths "over-the-Earth-limb", ionospheric delays were modeled using an exponential function of the height of ray path (HORP) above the Earth, which was based on ionospheric delays computed for each test orbit using the Bent ionospheric model. Receiver clock noise was simulated assuming a very high stability crystal oscillator with a 1-second root Allan variance of $0.16(10^{-9})$. A twice-integrated random walk model, which is based on [Brow 97], was used to simulate the clock bias and clock drift noise contributions.

3.2 – Navigation Performance Analysis Procedure

A Monte Carlo error analysis was performed for each of the three acquisition thresholds. Ensemble error statistics were accumulated for navigation solutions obtained by processing 50 sets of simulated pseudorange measurements that were created by the varying the random number seeds for the SA, random, and clock measurement errors. The GEODE flight software [GSFC 00] was used to compute the navigation solutions. Table 2 lists the GEODE processing parameters common to all cases. The navigation errors were computed by differencing the truth and estimated state vectors.

Table 2. GEODE Processing Parameters

| Parameter | Value |
|--|--|
| Nonspherical Earth Gravity model | 30x30 Joint Goddard Model (JGM)-2 |
| Solar and lunar ephemeris | Low-precision analytical ephemeris |
| Initial position error in each component | 100 to 1000 meters (consistent with point solution accuracy) |
| Initial velocity error in each component | 0.1 to 1 meter per second (consistent with point solution accuracy) |
| Initial solar radiation pressure coefficient error | HEO: 0.6 (40 percent) GEO: 0.042 (3 percent) |
| Initial receiver time bias error | 100 meters |
| Initial receiver time bias rate error | 0.1 meter per second |
| Estimated state | <ul style="list-style-type: none"> • User position and velocity • GPS receiver time bias and time bias drift • Solar radiation pressure coefficient |
| GPS SV ephemerides | Broadcast ephemerides for June 21-26, 1998 |
| Ionospheric editing | 500 kilometer minimum limb-crossing height |

4 – NAVIGATION PERFORMANCE FOR HIGHLY ECCENTRIC ORBIT

The HEO satellite was modeled as an inertially-pointing nanosatellite, with an area of 0.1 meters² and mass of 10 kilograms. The HEO receiving antenna model consists of two hemispherical antennas, one located on the top face of the satellite and one located on the bottom face, with boresights aligned parallel/antiparallel to the satellite spin axis, which is perpendicular to the ecliptic plane. Because of its high apogee and high perigee, its visibility of the GPS constellation is limited over the entire orbit. In addition, the antenna locations are not optimal for acquisition of GPS signals.

Fig. 2 shows the number of GPS SVs visible as a function of signal acquisition threshold and satellite altitude. The lower threshold cases have increased tracking of weaker signals from the side lobes of the GPS SV antenna pattern. Decreasing the signal acquisition threshold from 35 dB-Hertz to 30 dB-Hertz significantly increases the percent of time that at least one GPS SV is visible from 44 to 71 percent. Further decreasing the threshold to 28 dB-Hertz increases the percent of time that at least one GPS SV is visible to 78 percent. However, decreasing the signal acquisition threshold did not increase the maximum of two GPS SVs visible at apogee for this antenna configuration.

Fig. 3 compares the HEO ensemble true root-mean-square (RMS) errors for the three receiver acquisition thresholds for position and velocity. The ensemble true RMS error is defined as the RMS of the true error (difference between the estimated and the true state) at each time computed across all 50 Monte Carlo solutions. These results were obtained by processing measurements from all acquired GPS SVs every 3 minutes. Starting at perigee, approximately one orbit (23.5 hours) of processing was required to achieve steady-state performance. Starting at apogee, two perigee passages were required to achieve steady-state performance. Fig. 6 (presented in Section 6) provides the steady-state time-wise ensemble true RMS error statistics for this baseline case. These statistics are the RMS along the time axis of the ensemble true errors given in Fig. 3, omitting the initial convergence period.

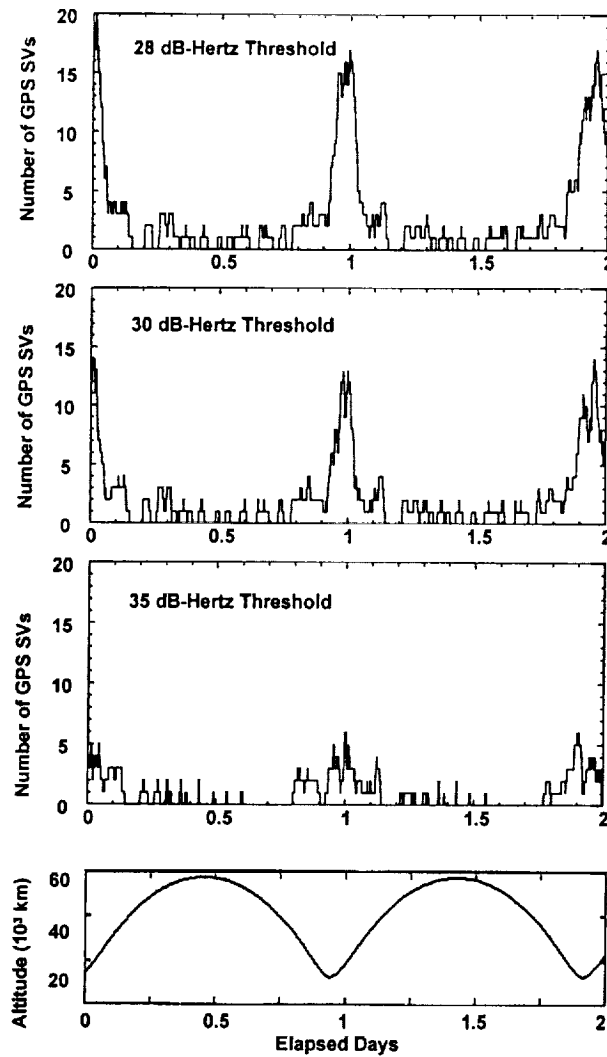


Fig. 2 GPS SV Visibility for the HEO Orbit

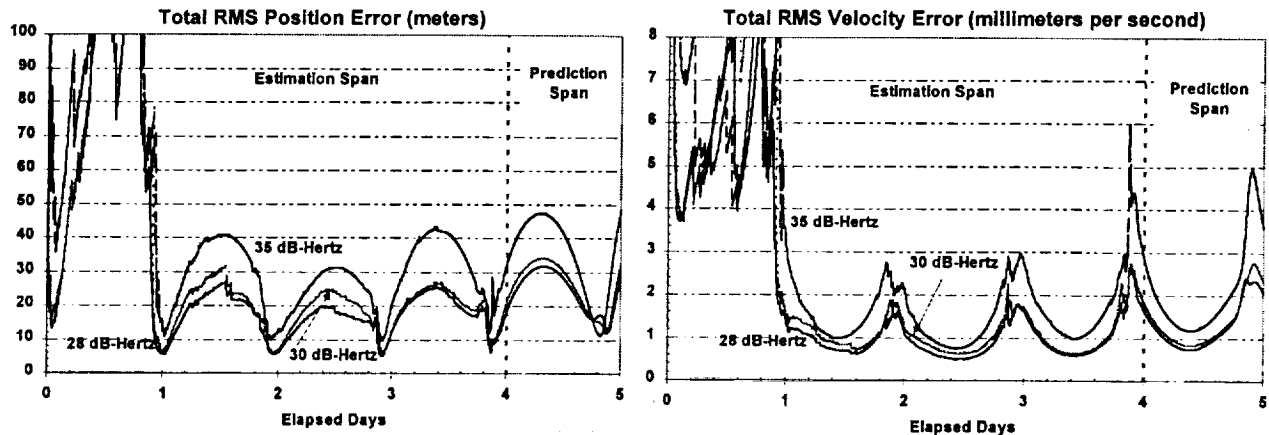


Fig. 3 Comparison of Ensemble True RMS Position and Velocity Errors for HEO

These analyses indicate that total position and velocity RMS accuracies of 30 meters and 2 millimeter per second can be achieved for the HEO orbit using a receiver with a high stability oscillator (see Table 1 for receiver clock noise characteristics) and a signal acquisition threshold of 35 dB-Hertz. The largest position errors occur near apogee and the smallest errors occur near perigee, where the GPS visibility is better. Decreasing the signal acquisition threshold from 35 to

30 dB-Hertz significantly reduces the total RMS position and velocity errors to about 20 meters and 1.2 millimeter per second, respectively. Decreasing the signal acquisition threshold from 30 to 28 dB-Hertz reduces the total RMS position and velocity errors to about 18 meters and 1.1 millimeter per second, respectively. The accuracy of the estimated clock bias improved from 17 meters (0.057 microsecond) RMS with the 35 dB-Hertz threshold to 12 meters (0.04 microsecond) and 10.5 meters (0.035 microsecond) with the 30 dB-Hertz and 28 dB-Hertz thresholds, respectively. In all cases, the prediction errors grow very slowly over a one-orbit prediction due to the high-fidelity orbit propagation model used in GEODE.

5 – NAVIGATION PERFORMANCE FOR GEOSYNCHRONOUS ORBIT

The GEO satellite configuration is based on GOES-10, with an area of 54 meters² and mass of 2100 kilograms. For the GEO satellite, the receiving antenna model consists of one nadir pointing high gain antenna. The satellite orbit is nearly circular, with a nearly constant altitude. Fig. 5 shows the resulting number of GPS SVs visible for the GEO satellite as a function of signal acquisition threshold. At this altitude, when the receiver has an acquisition threshold of 35 dB-Hertz, only GPS signals associated with the primary beam of the antenna pattern can be acquired. This region of visibility is small due to the interference of the Earth, as illustrated in Fig. 1. When the signal acquisition threshold decreases from 35 dB-Hertz to 30 dB-Hertz, signals from the side lobes of the GPS antenna pattern can be acquired, which increases the percent of time that at least one GPS SV is visible from 69 to 100 percent. Further decreasing the signal acquisition threshold to 28 dB-Hertz increases the percent of time that at least two GPS SV are visible to 100 percent.

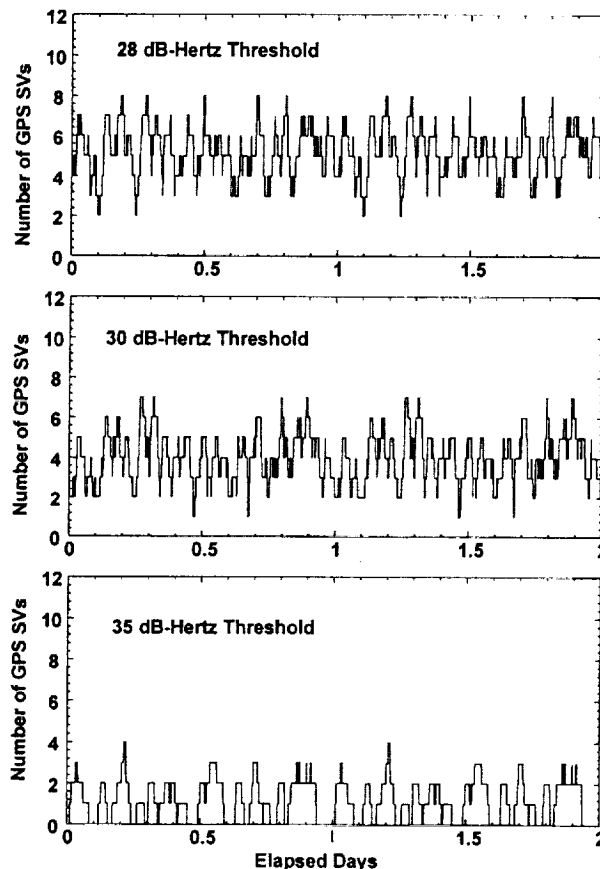


Fig. 4. GPS SV Visibility for the GEO Orbit

Fig. 5 compares the GEO steady-state ensemble true position and velocity RMS errors for the three acquisition thresholds, over the 4.5-day estimation span and a 1-day prediction span. Fig. 7 (presented in Section 6) summarizes the steady-state time-wise ensemble true RMS error statistics for this baseline case. These results were obtained by processing measurements from all acquired

GPS SVs every minute.

These analyses indicate that total position and velocity RMS accuracies of about 15 meters and 1 millimeter per second can be achieved for the GEO orbit using a receiver with a high stability oscillator (see Table 1 for receiver clock noise characteristics) and a signal acquisition threshold of 35 dB-Hertz. Decreasing the signal acquisition threshold from 35 to 30 dB-Hertz reduces the total RMS position and velocity errors to about 6 meters and 0.4 millimeter per second. Decreasing the signal acquisition threshold from 30 to 28 dB-Hertz reduces the total RMS position and velocity errors to about 5 meters and 0.35 millimeter per second. The accuracy of the estimated clock bias improved from 6 meters (20 nanoseconds) RMS with the 35 dB-Hertz threshold to 3 meters (10 nanoseconds) with the 30 dB-Hertz threshold and to 2.5 meters (8 nanoseconds) with the 28 dB-Hertz threshold. In all cases, the prediction errors grow very slowly over a one orbit prediction due to the high-fidelity orbit propagation model used in GEODE.

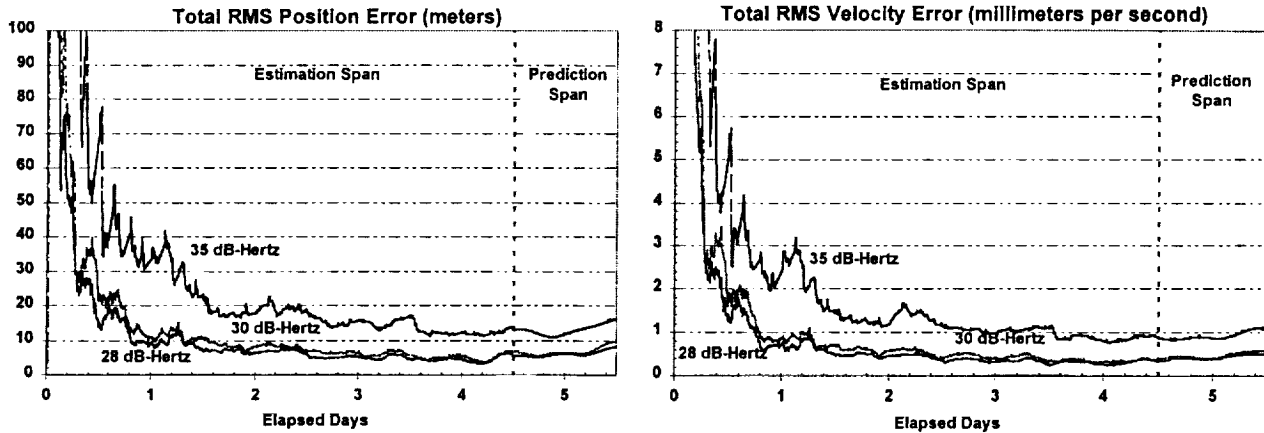


Fig. 5 Comparison of Ensemble True RMS Position and Velocity Errors for GEO

6 – NAVIGATION SENSITIVITY ANALYSIS

The sensitivity of the navigation accuracy for both the HEO and GEO test cases was investigated with respect to measurement errors and dynamic modeling errors. The results were very similar for both test cases. Fig. 6 and Fig. 7 summarize the sensitivity results for the HEO and GEO cases, respectively. In all cases simulated, reducing the receiver acquisition threshold from 35 to 30-dB-hertz threshold produced higher accuracy solutions that were less sensitive to errors. The additional improvement gained by reducing the acquisition threshold from 30 to 28 dB-hertz is small.

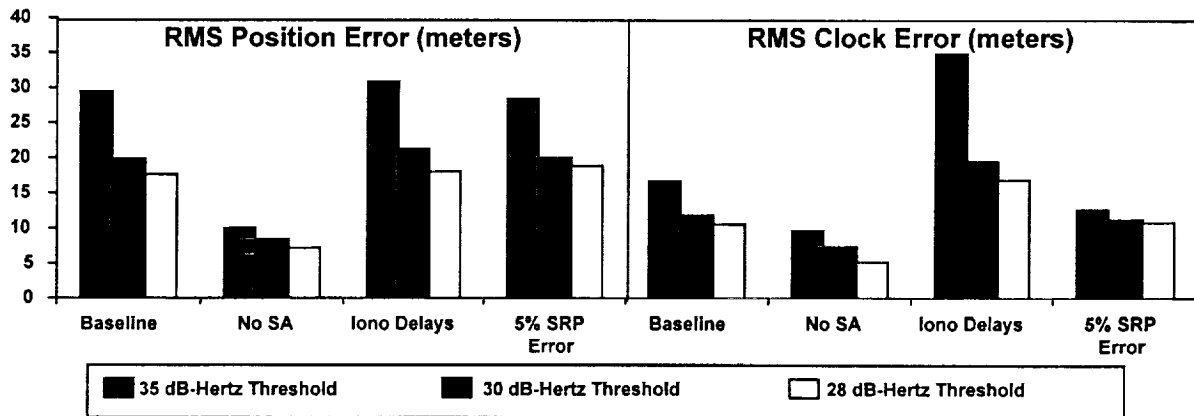


Fig. 6. Comparison of Steady-State Time-Wise Ensemble RMS True Errors for HEO

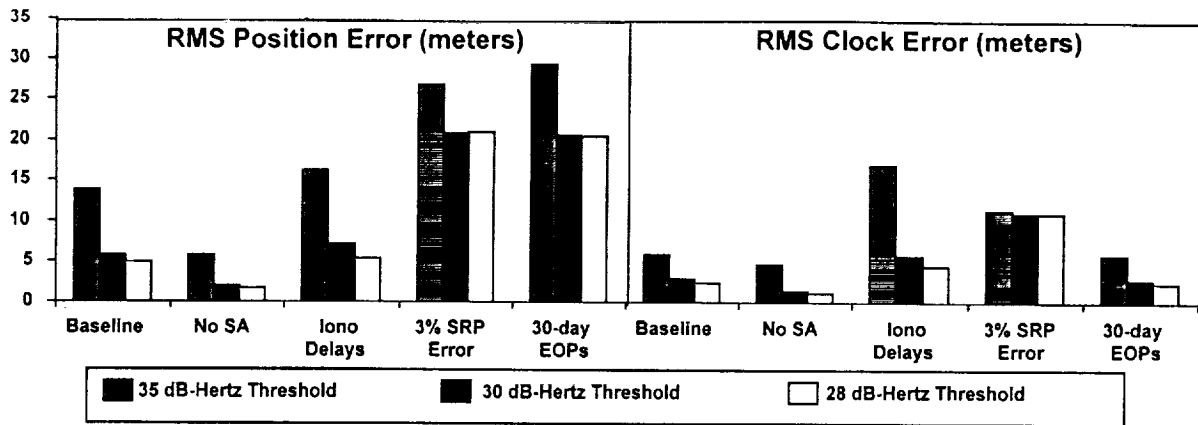


Fig. 7. Comparison of Steady-State Time-Wise Ensemble RMS True Errors for GEO

Using a GPS receiver with a high stability oscillator, SA error was found to be the primary measurement-related error contributor. When SA errors were removed, solution errors decreased by more than 50 percent (No SA). The inclusion of measurements with large ionospheric delays was the next largest measurement-related contributor, producing significant biases in the clock bias estimates particularly for the 35-dB-hertz acquisition threshold (29 meters for HEO and 11 meters for GEO) (Iono Delays). In addition, the error variations with time were more erratic for all parameters when the measurements with large ionospheric delays were processed, indicating poorer quality solutions. The impact of random measurement error was much smaller than SA or ionospheric effects.

For high Earth orbits, the primary dynamic modeling errors arise from unmodeled variations in the solar radiation pressure acceleration and errors in the predicted Earth orientation parameters used in the transformation from the GPS Earth-Centered Earth-Fixed frame to an inertial frame. Starting with an initial solar radiation pressure coefficient error of 40 percent for the baseline HEO case, the solar radiation pressure correction was estimated to within about 5 percent. Starting with an initial solar radiation pressure coefficient error of 3 percent for the baseline GEO case, the solar radiation pressure correction was estimated to within about 0.1 percent. To assess the impact of uncorrected errors in the solar radiation pressure coefficient, Monte Carlo simulations were performed in which the initial value of the solar radiation pressure coefficient was offset but a correction was not estimated. For the HEO with a small area to mass ratio (0.01 meters² per kilogram), an uncorrected 5 percent error in the solar radiation pressure coefficient (5% SRP Error) did not degrade the solution; however an uncorrected 10 percent error produced significantly larger errors. For the GEO satellite with a larger area to mass ratio (0.026 meters² per kilogram), an uncorrected 3 percent solar radiation pressure error (3% SRP Error) significantly degraded the performance, particularly for the in-track position and clock bias. This indicates that, if the error in the solar radiation pressure force is significant, the solar radiation pressure coefficient should be estimated. However, if the solar radiation pressure error is not observable, attempting to estimate it can degrade the solution. Simulations using 30-day predicted values of the Earth orientation parameters distributed by the International Earth Rotation Service also showed significant increases in the solution errors, indicating that up-to-date values for the UT1-UTC time differences should be commanded on weekly basis for best performance (30-day EOPs).

In all cases simulated, the HEO case required two perigee passages for convergence because of its poor GPS visibility near apogee. Convergence for the GEO cases was considerably faster when using a receiver with a 30- or 28-dB-hertz threshold. Elimination of SA measurement errors significantly reduced the convergence time for the GEO case when using a receiver with a 35-dB-hertz threshold. Estimation of an accurate solar radiation pressure correction required approximately one orbital period, regardless of the receiver threshold.

7 – CONCLUSIONS AND FUTURE DIRECTIONS

This study demonstrates the feasibility of using GPS for high accuracy navigation of satellites in HEO and GEO orbits and indicates that navigation accuracy and stability can be improved by reducing the acquisition threshold in the receiver. A navigation accuracy of better than 30 meters RMS is achievable using a GPS receiver with a highly stable oscillator and a 35-dB-Hertz acquisition. This accuracy improves to better than 20 meters RMS by reducing the acquisition threshold by only 5 dB-hertz. In the future when SA is disabled, an accuracy of better than 2 meters RMS will be achievable using a receiver with the reduced acquisition threshold. When using a GPS receiver with a high stability clock, the primary factors impacting navigation performance for high-Earth orbiting satellites are (1) the quality of GPS visibility, characterized by the number of GPS SVs that can be simultaneously acquired and the length of the time period when no GPS SVs can be acquired, (2) SA measurement errors, (3) large uncorrected ionospheric delays in the processed measurements, and (4) dynamic modeling errors.

The performance results presented in this paper are optimistic due to the simulation of measurement errors characteristic of a GPS receiver with a highly stable oscillator. Therefore, future directions will include a detailed investigation of the impact of using a GPS receiver with a lower stability oscillator. This will require more realistic modeling of the behavior of the actual oscillator specified for the PiVoT receiver, validated by experimental tests in a thermal-vacuum chamber. Expectations are that the navigation performance is particularly sensitive to the level of the drift noise, due to long periods of time without visible GPS SVs (up to 7 hours for the HEO case with a 35 dB-Hertz threshold). Navigation performance will be assessed for spacecraft orbits with even poorer SV visibility, e.g., the 10x50 Earth radii orbit proposed for the Magnetospheric Multiscale mission. In addition, alternate approaches to reduce/eliminate the impact of large ionospheric delays will be investigated such as estimating pseudorange measurement biases for each GPS SV and estimating scaling parameters in an ionospheric delay model. Initialization algorithms that can be used when fewer than four GPS SVs are acquired will also be defined and evaluated. The impact of the initial errors larger than 1 kilometer and 1 meter per second on the convergence of the extended Kalman filter estimator will also be investigated.

REFERENCES

- [Brow 97] R. G. Brown and P. Y. C. Hwang, *Introduction to Random Signals and Applied Kalman Filtering*, Third Edition, John Wiley and Sons, 1997
- [Godd 00] Goddard Space Flight Center, CSC-96-968-01R0UD1, *Global Positioning System (GPS) Enhanced Orbit Determination (GEODE) Mathematical Specifications, Version 5*, T. Lee and A. Long (CSC), prepared by Computer Sciences Corporation, February 2000
- [Gram 94] C. J. Gramling et al., "TDRSS Onboard Navigation System (TONS) Flight Qualification Experiment," *Proceedings of the Flight Mechanics/Estimation Theory Symposium 1994*, NASA Conference Publication 3265, May 17-19, 1994, p.253-267
- [Hart 97] R. Hart, A. Long, and T. Lee, "Autonomous Navigation of the SSTI/Lewis Spacecraft Using the Global Positioning System (GPS)," *Proceedings of the Flight Mechanics Symposium 1997*, NASA Conference Publication 3345, May 19-21, 1997, p.123-133
- [JSC 93] Johnson Space Center, *Range Bias Models for GPS Navigation Filters*, W. M. Lear, Charles Stark Draper Laboratory, June 1993
- [Land 98] R. Landry, Jr. et al., "Studies on Acquisition and Tracking Threshold's Reduction for GPS Spaceborne and Aeronautical Receivers," *Proceedings of the ION GPS 98*, Nashville, Tennessee, pp 619-624
- [More 99] M. Moreau et al., "GPS Receiver Architecture and Expected Performance for Autonomous GPS Navigation in Highly Eccentric Orbits," *Proceedings of the 55th Annual ION Meeting*, Cambridge Massachusetts, June 28-30, 1999